Wind-resistant performance of cable-supported bridges using carbon fiber reinforced polymer cables

Xin-Jun Zhang[†] and Lei-Dong Ying

College of Civil Engineering and Architecture, Zhejiang University of Technology, Hangzhou 310032, P.R. China

Abstract. To gain understanding of the applicability of carbon fiber reinforced polymer (CFRP) cable in cable-supported bridges, based on the Runyang Bridge and Jinsha Bridge, a suspension bridge using CFRP cables and a cable-stayed bridge using CFRP stay cables are schemed, in which the cable's cross-sectional area is determined by the principle of equivalent axial stiffness. Numerical investigations on the dynamic behavior, aerostatic and aerodynamic stability of the two bridges are conducted by 3D nonlinear analysis, and the effect of different cable materials on the wind resistance is discussed. The results show that as CFRP cables are used in cable-supported bridges, (1) structural natural frequencies are all increased, and particularly great increase of the torsional frequency occurs for suspension bridges; (2) under the static wind action, structural deformation is increased, however its aerostatic stability is basically remained the same as that of the case with steel cables; (3) for suspension bridge, its aerodynamic stability is superior to that of the case with steel cables, but for cable-stayed bridge, it is basically the same as that of the case with steel stay cables. Therefore as far as the wind resistance is considered, the use of CFRP cables in cable-supported bridges is feasible, and the cable's cross-sectional area should be determined by the principle of equivalent axial stiffness.

Keywords: cable-supported bridges; carbon fiber reinforced polymer cable; dynamic behavior; aerostatic stability; aerodynamic stability.

1. Introduction

By the end of the last century, the Akashi Kaikyo Bridge (1990 m) in Japan and the Great Belt Bridge (1624 m) in Denmark represent outstanding achievements in building suspension bridges with a span approaching 2000 m. Meanwhile, the Normandy Bridge (856 m) in France and the Tatara Bridge (890 m) in Japan made cable-stayed bridge to compete with suspension bridge for spans over 1000 m. Into the 21st century, world's bridge construction is entering into a new era of building the sea-crossing and island-linking projects. To meet with the navigation requirement and overcome the construction difficulty of deep-water foundation, longer and longer span of cable-supported bridges are being planned, such as the Messina bridge (3300 m) in Italy and the Gibraltar bridge between Spain and Morocco (3550 m) for suspension bridges (Astiz 1998), for cable-stayed bridges such as the Stonecutters Bridge (1018 m) in Hong Kong and the Sutong Bridge (1088 m) in

† PhD, Professor, Corresponding Author, E-mail: xjzhang@zjut.edu.cn

China (Xiang and Ge 2002).

With the rapid increase of span length, the bridges are becoming lighter, slender and more sensitive to the wind action, and some new problems are arising. One of the most important of these is structural design. Generally, the design of super long-span suspension bridges is mainly controlled by structural dead load, and the cables contribute a large portion to structural dead load. Therefore, using of the materials with higher tensile strength and lower mass density for the cables can decrease the cable's dead load, save the cable's materials and decrease the dimensions of substructures, and finally decrease the cost and construction difficulty for suspension bridges. For cable-stayed bridges, the stay cables are also important structural elements, and they have significant influences on structural performance and appearance. At present, the stay cable is commonly made of traditional steel wires. On the structural performance, the steel cable is relatively heavy, resulting in significant sagging effect due to its self-weight, thus reducing the effective stiffness of the stay cable and making it behave softer under service load. In addition, for the tradition steel cable, corrosion and fatigue are two major problems in bridges with high traffic volume or bridges located in corrosion environment, which cause the premature rupture of the wires inside the cable. Moreover, the cost of replacement and maintenance of the steel cable is generally high.

Continuous attempts are making to improve the traditional cable's materials, at the same time engineers and researchers try to develop new engineering materials. Among them, more attentions are attracted to the CFRP material. Compared to the traditional cable material of high strength steel, the CFRP has the properties of about 2 times higher in tensile strength, about 80% of the elastic modulus, only about 20% of the mass density of steel and other outstanding advantages including excellent corrosion-resistant and fatigue-resistant ability, and low thermal expansion coefficient etc. (Chen 1999). Although the CFRP material has a high cost and low shear capacity, with the increase of production and development of new anchorage system, these problems are being solved, and the CFRP material is believed to have the greatest potential application prospect. At present, the CFRP material is widely used in the seismic retrofit and rehabilitation of existing concrete bridges. Due to the fact that the CFRP has the highest modulus-density ratio among the available structural materials, it is most suitable for application as structural members where maximum stiffness and minimum weight are required, such as the cables in cable-stayed and suspension bridges. Its high stiffness-mass density ratio can reduce the longitudinal deformation of the cables under loads and the sagging effect due to the self-weight. The outstanding fatigue resistant property of CFRP also satisfies the typical loading conditions of the cable-stayed bridge consisting large cyclic load amplitudes. The excellent corrosion resistance of CFRP makes it more economical for maintenance as compared to steel. Therefore, the feasibility of using CFRP cables in long-span cable-supported bridges attracts increasing attentions from civil engineers (Hojo and Noro 2002, Kim and Meier 1991, Meier 1992,1996,1999, Noistering 2000, Ohashi 1991). The first application of CFRP cables in a real cable-stayed bridge is the Stork Bridge in Switzerland in 1996, but only two of the 24 cables are made of CFRP (Chen 1999). A few of cable-stayed pedestrian bridges with CFRP stay cables have been successfully built for research purpose such as the Herning Footbridge in Denmark (Kremmidas 2004), the Laroin Footbridge in France (Geffroy 2002) etc. Also, some cable-stayed bridges with CFRP stay cables have been proposed as design alternatives such as the I-5/Gilman Advanced Technology Bridge in America (Kremmidas 2004) etc. But for suspension bridges, the real application of CFRP material as main cables has not been reported until now.

Comprehensive studies on the material and mechanics performance, economy, construction, anchorage system etc of the CFRP cable have been done in analytical and test manners (Gaubinger

and Kollegger 2002, Kremmidas 2004). Some investigations on the static and dynamic behavior, economy, and wind resistance of cable-stayed bridges using CFRP stay cables also have been conducted by Chen (1999), Kremmidas (2004), Kou and Xie (2005) etc. However, very little research on the availability of using CFRP cables in suspension bridges has been conducted. For long-span suspension bridges, increasing structural dead load can greatly improve their gravity stiffness, and thus the static and dynamic behavior. Therefore, using of CFRP material with lower elastic modulus and mass density as main cables seems to be not advisable. As the bridges become longer and longer, whether or not the wind resistance of cable-supported bridges becomes worse needs to be further investigated. In this work, based on the Runyang Bridge and Jinsha Bridge, a suspension bridge using CFRP cables and a cable-stayed bridge using CFRP stay cables are schemed. Numerical investigations on the dynamic behavior, aerostatic and aerodynamic stability of the two bridges are conducted by 3D nonlinear analysis, and the feasibility of using CFRP cables in suspension and cable-stayed bridges is also discussed based on the wind resistance.

2. Suspension bridge

2.1. Description of the sample bridge

In this work, the Runyang Bridge is taken as example, which is the longest suspension bridge as of 2005 in China. The bridge has a 1490 m main span and two 470 m side spans, as shown in Fig. 1 (Chen and Song 2000). The cable's sag to span ratio is 1/10, and the spacing of two cables is 34.3 m. The deck is a steel streamlined box girder with 3.0 m high and 35.9 m wide. The concrete door-shaped towers are about 209 m high. For the purpose of discussion, a same span length of suspension bridge with CFRP cables is schemed. Except for the material and sectional properties of the cables and hangers, other design parameters of the two bridges are remained the same. Structural material and sectional properties of the two cases are presented in Table 1. In the
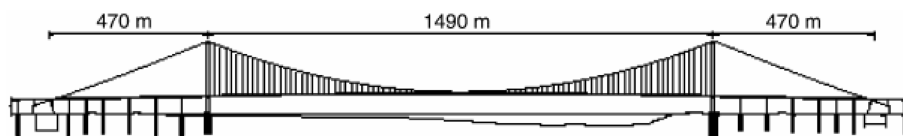

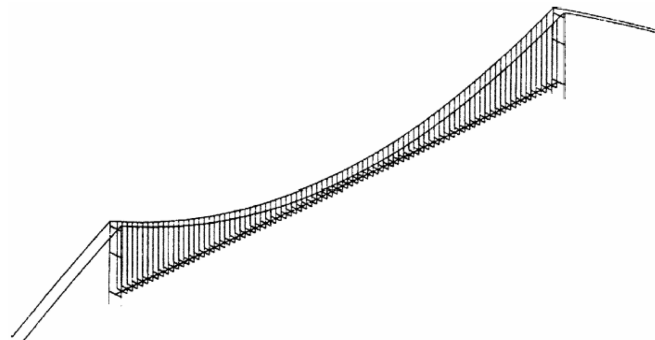Fig. 1 General layout of the Runrang Bridge

Fig. 2 Three-dimensional finite element model of the Runyang Bridge

Table 1 Structural material and sectional properties

Members		E (Mpa)	A (m^2)	J_d (m^4)	I_z (m^4)	I_y (m^4)	M (kg/m)	J_m (kg·m^2/m)
Deck		2.1×10^5	1.2481	5.034	1.9842	137.7541	18386.5	1.852×10^6
Cable	Steel	2.0×10^5	0.47347	-	-	-	3817.4	-
	CFRP	1.65×10^5	0.5739	-	-	-	895.3	-
Hanger	Steel	2.0×10^5	0.00214	-	-	-	16.8	-
	CFRP	1.65×10^5	0.00259	-	-	-	4.0	-

Note: E = elastic modulus, A = cross-sectional area, J_d = torsional moment of inertia, I_z = vertical bending moment of inertia, I_y = lateral bending moment of inertia, M = mass per unit length, J_m = mass moment of inertia per unit length.

following analysis, the bridge is idealized to a 3D finite element model as shown in Fig. 2, in which the deck and towers are modeled by 3D beam elements, and the hangers and cables are modeled by 3D bar elements, and rigid beams are provided to model the connections between the deck and the hangers.

The cross-sectional areas of CFRP cables and hangers as presented in Table 1 are determined by the equivalent axial stiffness, and calculated by the following equation (Chen 1999) :

$$E_{CFRP}A_{CFRP} = E_{Steel}A_{Steel} \tag{1}$$

Where E_{CFRP}, E_{Steel} are the elastic modulus of CFRP and steel respectively; A_{CFRP}, A_{Steel} are the cross-sectional areas of CFRP and steel cables respectively.

2.2. Dynamic behavior

On the equilibrium position of the bridge in completion, the first 20 modes of the bridge using either CFRP or steel cables are calculated by the dynamic characteristics finite element analysis, in which the subspace iteration method is adopted and structural geometric nonlinearity is also

Table 2 Effect of cable materials on structural natural frequencies (Hz)

Mode type	Cable type		Mode shape
	Steel	CFRP	
Vertical bending	0.1260	0.1305	1st, symmetric
	0.0999	0.1033	1st, antisymmetric
	0.1723	0.1875	2nd, symmetric
	0.1898	0.1925	2nd, antisymmetric
	0.2427	0.2476	3rd, symmetric
	0.2916	0.2970	3rd, antisymmetric
Lateral bending	0.04979	0.0508	1st, symmetric
	0.1249	0.1278	1st, antisymmetric
Torsion	0.2410	0.3123	1st, symmetric
	0.2408	0.3153	1st, antisymmetric

considered (Zhang, *et al.* 2002). Table 2 shows the natural frequencies of the first three vertical bending modes, the first lateral bending and torsional modes.

As CFRP cables are used, the natural frequencies of both vertical and lateral bending modes are increased by less than 9% as compared to the case of using steel cables, and particularly the torsional frequency is remarkably increased by 29.6%. The fact can be mainly attributed to the decrease of structural mass. The mass of the bridge is about 26020 kg/m in the case of steel cables, whereas in the case of CFRP cables, it is about 20180 kg/m, and decreased by 22.4%. Similarly, the mass moment of inertia of the bridge is about 2.97×10^6 kg·m^2/m in the case of steel cables, whereas in the case of CFRP cables, it is about 2.12×10^6 kg·m^2/m, and decreased by 28.6%. Because the CFRP cable is designed by the principle of equivalent axial stiffness, structural stiffness under the two cases is almost the same. With the same stiffness and much lower mass and mass moment of inertia, structural natural frequencies are therefore increased. The adoption of CFRP cables in the Runyang Bridge has the effect of stiffening the structure by increasing its natural frequencies.

2.3. Aerostatic behavior

As known from the wind tunnel test, the bridge is prone to wind instability under the positive wind attack angle (Chen and Song 2000). Therefore in the following analyses, the common wind attack angles of 0° and +3° are selected. With the increase of wind speed, aerostatic behaviors of the Runyang Bridge with either CFRP cables or steel cables are investigated by three-dimensional nonlinear aerostatic analysis (Zhang, *et al.* 2002). In the analysis, the drag, lift and twist moment components of the aerostatic load are considered for the deck, and the corresponding aerostatic coefficients are obtained from the sectional-model wind tunnel test (Chen and Song 2000), as shown in Fig. 3; for the cables, hangers and towers, only the drag component is considered, and the corresponding drag coefficient is 0.7 for the cables and hangers and 2.0 for the towers. Variations of the deck's displacements at midspan with wind speed under wind attack angle of 0° and +3° are plotted in Fig. 4 and Fig. 5 respectively.

In the case of CFRP cables, as compared to the case of steel cables, the lateral, vertical and torsional displacements are all increased as shown in Fig. 4 and Fig. 5. At the low wind speed, structural deformations are almost the same for both two cases. However, the difference is increased with the growth of wind speed. The increase of structural deformation, on the one hand, can be attributed to the increase of drag component acting on CFRP cables. As presented in Table 1, the
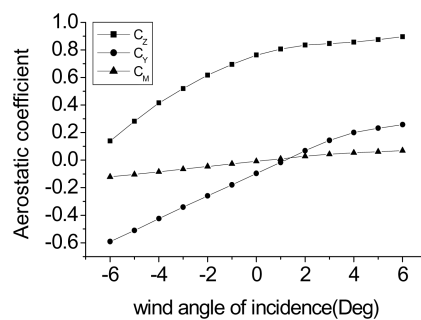

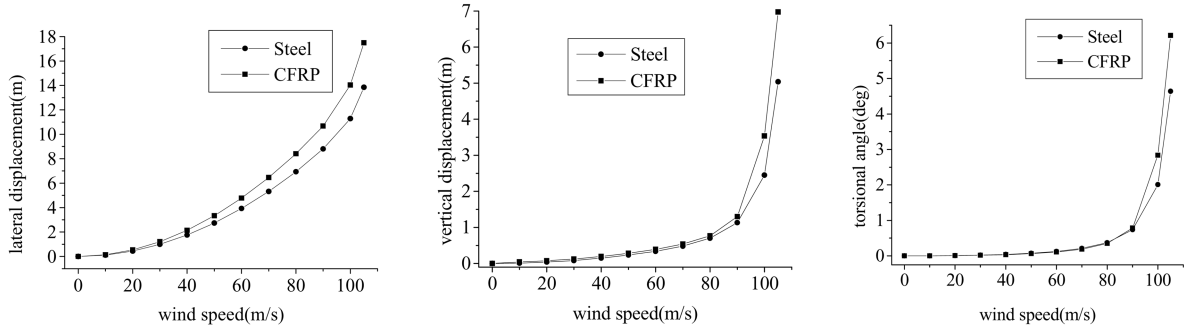Fig. 3 Aerostatic coefficients versus wind angle of incidence

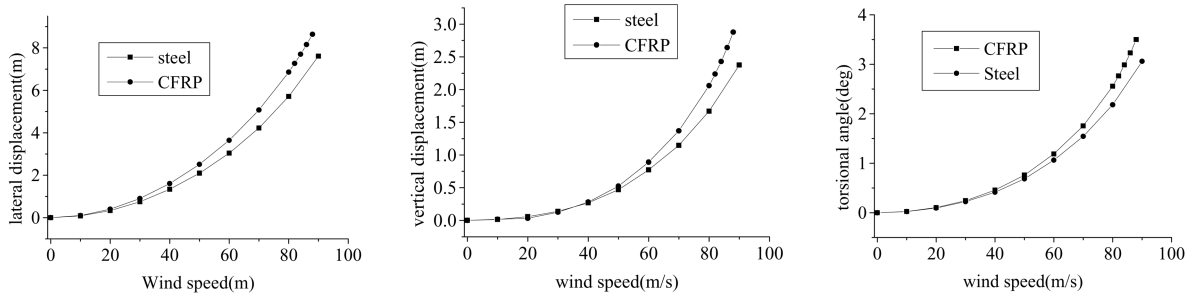Fig. 4 Variations of the deck's displacements at midspan with wind speed under wind attack angle of 0°

Fig. 5 Variations of the deck's displacements at midspan with wind speed under wind attack angle of +3°

ratio of elastic modulus between steel and CFRP is 1.212, the cross-sectional area of CFRP cable determined by the principle of equivalent axial stiffness is therefore 1.212 times that of the steel cable, the cable's diameter is increased from 0.474 m to 0.574 m, and increased by 21.1%. With the increase of vertical projected height, the drag component of aerostatic load is increased consequently, which leads to the greater structural deformation. On the other hand, it is might due to the decrease of structural gravity stiffness when replacing lighter CFRP cables for steel cables.

Under wind attack angle of 0° as plotted in Fig. 4, as wind speed is over 90 m/s, the vertical and torsional displacements are increased sharply for both two cases. It means that the critical condition of aerostatic instability is reached. Therefore, the critical wind speeds of aerostatic stability for both two cases are identical. However under wind attack angle of +3° as plotted in Fig. 5, the evolutions of structural displacements with wind speed are obviously different from that in the case of 0°. Sharp changes of the displacement curves do not happen, but the slopes of displacement curves are increased remarkably with the growth of wind speed. In the case of using CFRP cables, structural nonlinear analysis is not divergent at the wind speed of 88 m/s, which means that the bridge is under the critical condition of aerostatic instability. Similarly at this wind speed, the divergence of aerostatic analysis becomes difficult for the bridge with steel cables. Therefore, the critical wind speeds of aerostatic instability are also remained the same for the two bridge under this wind attack angle.

It is concluded from the above analysis that compared with the bridge with steel cables, greater displacements are caused by the static wind action, however the critical wind speed of aerostatic instability is basically the same. Therefore viewed from the aspect of aerostatic stability, the use of CFRP cables in long-span suspension bridges is feasible.
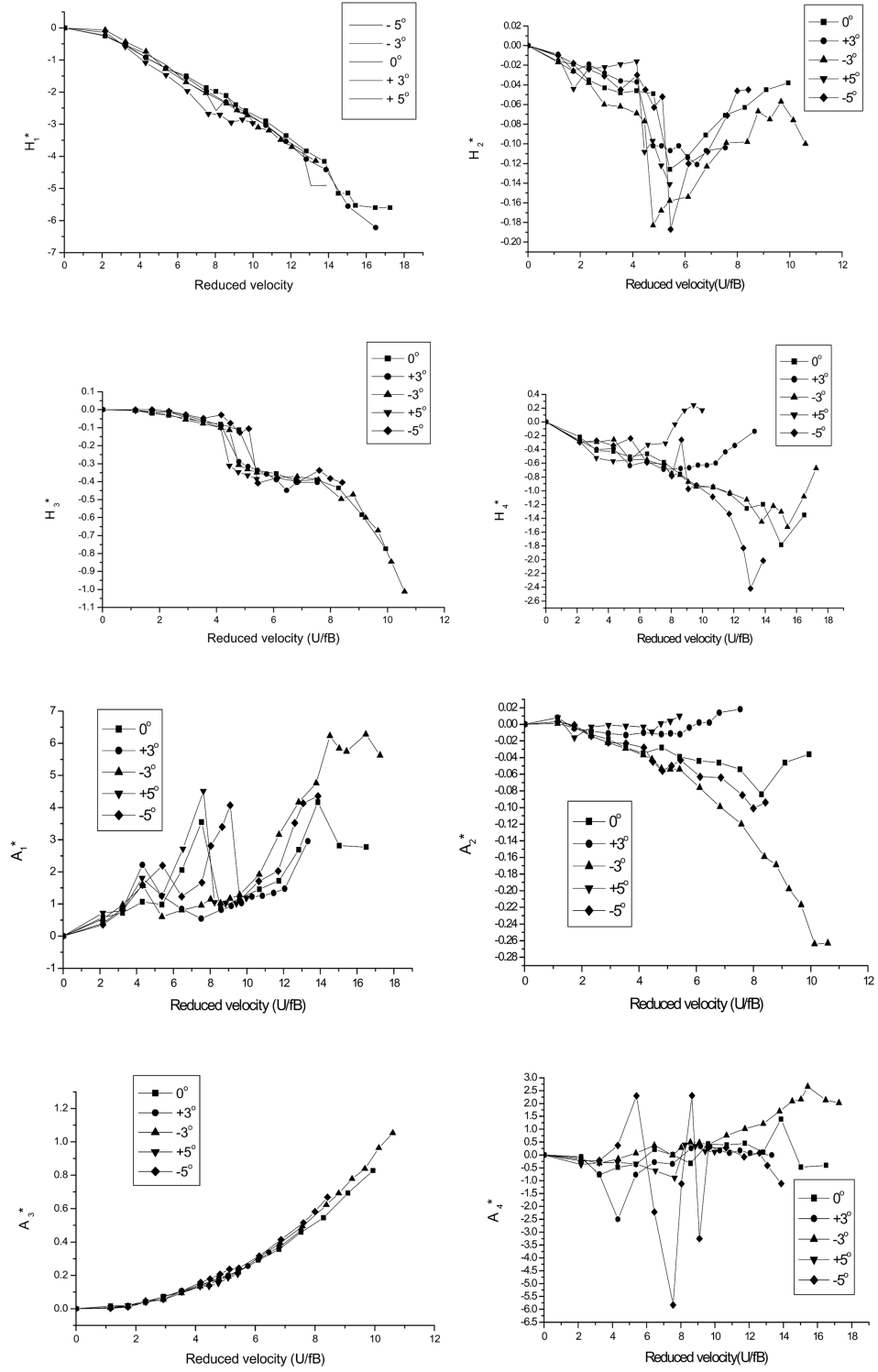
Fig. 6 Flutter derivatives at varying angles of wind incidence versus the reduced velocity

Table 3 Effect of cable materials on the critical wind speed (m/s)

Wind attack angle	Cable type	
	Steel	CFRP
+3°	40.1	47.0
0°	69.6	79.9

2.4. Aerodynamic stability

Under wind attack angles of 0° and +3°, aerodynamic stability of the bridge with CFRP and steel cables is investigated by three-dimensional nonlinear aerodynamic stability analysis (Zhang, *et al.* 2002), and the critical wind speeds of aerodynamic instability are presented in Table 3. In the analysis, the deck's aerodynamic derivatives as shown in Fig. 6 are obtained from the sectional-model wind tunnel test of the bridge (Chen and Song 2000), the first 20 modes are involved, and the modal damping ratio is taken as 0.5%.

In the case of CFRP cables used, the critical wind speeds are greatly increased. The increase amplitude is 17.2% under wind attack angle of +3°, and under wind attack angle of 0°, it is 14.8%. Therefore viewed from the aerodynamic stability, the CFRP cables is confirmed analytically to be superior to the case of steel cables. The improvement of aerodynamic stability can be explained from the simplified formula of critical wind speed expressed as

$$V_{cr} = \eta_s \cdot \eta_\alpha \cdot V_{c0}, \qquad V_{c0} = 2.5 \cdot C \cdot f_t \cdot B$$

$$C = \sqrt{\mu \cdot \frac{r}{b}}, \qquad \mu = \frac{m}{\pi \rho b^2}, \qquad b = \frac{B}{2}, \qquad r = \sqrt{\frac{I_m}{m}} \tag{2}$$

where η_s is the modified coefficient of cross section shape; η_α is the modified coefficient of wind attack angle; V_{c0} is the critical wind speed of the coupled flutter of a thin plate; f_t is the fundamental torsional frequency; B is the width of the deck; μ is the density ratio of the bridge to air; m is the mass of the deck and cables per unit length; ρ is the mass density of air; I_m is the mass inertia of the deck and cables per unit length.

As CFRP cables are used, due to the remarkable reductions of the mass and mass moment of inertia of the bridge, the coefficient C is therefore decreased by 13.7%. However as given in Table 2, the increase in the fundamental torsional frequency is more than 2 times of reduction of the coefficient C, and therefore the critical wind speed is increased. Viewed from the aspect of aerodynamic stability, the use of CFRP cables in long-span suspension bridges is also feasible.

3. Cable-stayed bridge

3.1. Description of the sample bridge

The Jingsha Bridge is a three-span cable-stayed bridge with a 500 m center span and two 200 m side spans as shown in Fig. 7 (Song 1998). The deck is Π-shaped, 27.0 m wide and 2.0 m high. The H-shaped towers are 137 m high. Two cable planes are inclined and fan-shaped. In the following analysis, the bridge is idealized to a three-dimensional finite element model as plotted in Fig. 8, in which the columns and transverse beams of towers and the girder are modeled by 3D beam elements, and the stay
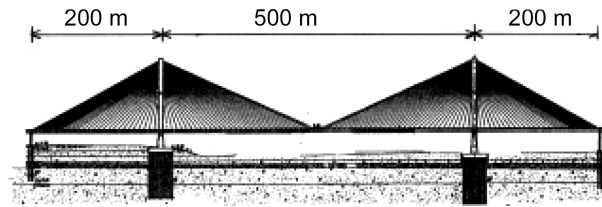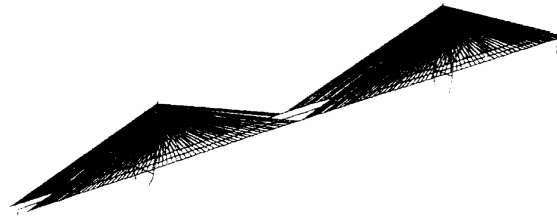
Fig. 7 General view of the Jingsha Bridge

Fig. 8 Three-dimensional finite element model of the Jingsha Bridge

Table 4 Effect of cable materials on structural natural frequencies (Hz)

Mode No	Cable type		Mode shape
	Steel	CFRP	
2	0.1841	0.1870	1st symmetric vertical bending
3	0.2472	0.2510	1st antisymmetric vertical bending
4	0.3520	0.3576	1st symmetric lateral bending
5	0.3951	0.4065	1st symmetric torsion
6	0.4435	0.4557	2nd symmetric vertical bending
9	0.5105	0.5164	2nd antisymmetric vertical bending
10	0.5202	0.5332	1st antisymmetric torsion

cables are modeled by 3D bar elements. The deck is idealized to a three-girder finite element model. The connections between the bridge components and the supports are properly modeled.

3.2. Dynamic behavior

On the equilibrium position of the bridge in completion, the first 10 modes of the bridge using either CFRP or steel stay cables are computed by the dynamic characteristics finite element analysis, in which the subspace iteration method is adopted and structural geometric nonlinearity is also considered (Zhang, *et al*. 2002). Table 4 shows the modal properties of the deck.

As CFRP stay cables are used, the natural frequencies of all modes are increased by less than 5% as compared to the case of steel stay cables. The fact can be mainly attributed to the decrease of structural mass. Because the CFRP stay cable is designed by the principle of equivalent axial stiffness, structural stiffness under the two cases is basically the same, but the mass per unit length of the CFRP stay cable is only 0.235 times that of the steel stay cables. With the same stiffness and much lower mass and mass moment of inertia, the natural frequencies are therefore increased. The adoption of

CFRP stay cables has the effect of stiffening the structure by increasing its natural frequencies.

3.3. Aerostatic behavior

As known from the wind tunnel test, the bridge is prone to wind instability under the negative wind attack angle. Therefore in the following analyses, the wind attack angles of 0° and -3° are selected. With increase of wind speed, aerostatic behaviors of the bridge with either CFRP or steel stay cables are investigated by three-dimensional nonlinear aerostatic analysis (Zhang, *et al*. 2002). In the analysis, the drag, lift and twist moment components of the aerostatic load are considered for the deck, and the corresponding aerostatic coefficients are obtained from the sectional-model wind tunnel test (Song 1998), as shown in Fig. 9; for the stay cables and towers, only the drag component is considered, and the corresponding drag coefficient is 0.7 for the stay cables and 2.0
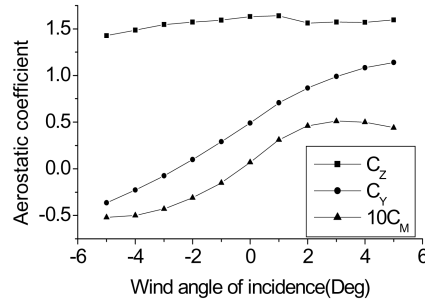

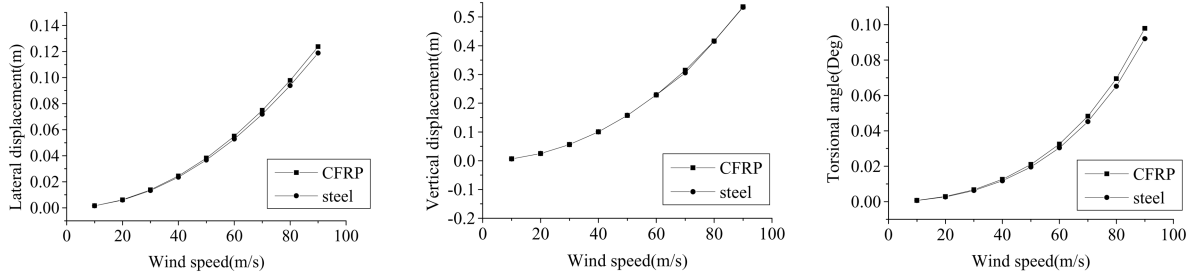Fig. 9 Aerostatic coefficients versus wind angle of incidence

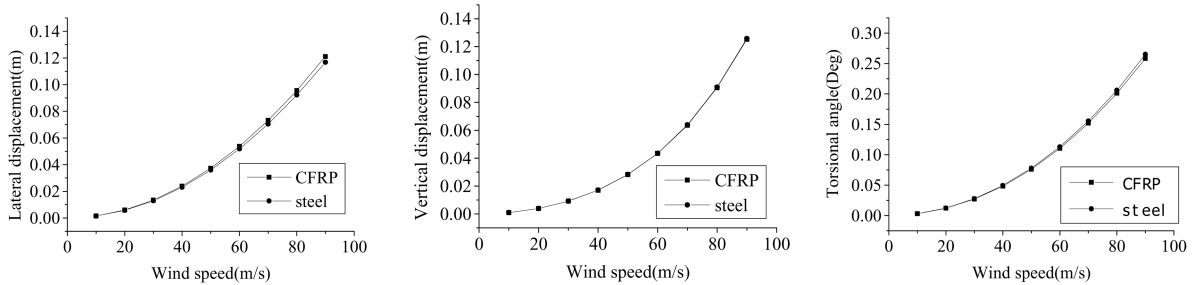Fig. 10 Variations of the deck's displacements at midspan with wind speed under wind attack angle of 0°

Fig. 11 Variations of the deck's displacements at midspan with wind speed under wind attack angle of -3°

for the towers. Variations of the deck's displacements at midspan with wind speed under wind attack angle of $0°$ and $-3°$ are plotted in Fig. 10 and Fig. 11 respectively.

In the case of CFRP stay cables used, as compared to the case of steel cables used, the lateral, vertical and torsional displacements are all slightly increased as shown in Fig. 10 and Fig. 11. At the low wind speed, structural deformations are almost the same for both two cases. However, the difference is increased with the growth of wind speed. The increase of structural deformation can be attributed to the increase of drag component acting on CFRP stay cables. Compared to the steel stay cable, the cross-sectional area of CFRP stay cable is increased by 18.2%, and the stay cable's diameter is thus increased 8.72%. With the increase of vertical projected height, the drag component of aerostatic load is increased consequently, which leads to the greater structural deformation. On the whole, the difference of structural displacements between the two cases is very little. Therefore, it can be concluded that the critical wind speed of aerostatic instability is basically the same for the two cases. Therefore viewed from the aspect of aerostatic stability, the use of CFRP stay cables in long-span cable-stayed bridges is feasible.

3.4. Aerodynamic stability

Under wind attack angles of $0°$ and $±3°$, aerodynamic stability of the bridge with CFRP and steel stay cables is investigated by three-dimensional nonlinear aerodynamic stability analysis (Zhang, *et al*. 2002), and the critical wind speeds of aerodynamic instability are presented in Table 5. In the analysis, the deck's aerodynamic derivatives as shown in Fig. 12 are obtained from the sectional-model wind tunnel test of the bridge (Song 1998), the first 10 modes are involved, and the modal damping ratio is taken as 1.0%.

In the case of CFRP stay cables used, the critical wind speed is decreased, but the decrease is very limited. The fact can be also explained by Eq. (2). Due to the decrease of structural mass, structural frequencies are slightly increased, as shown in Table 4. Because the increase of the
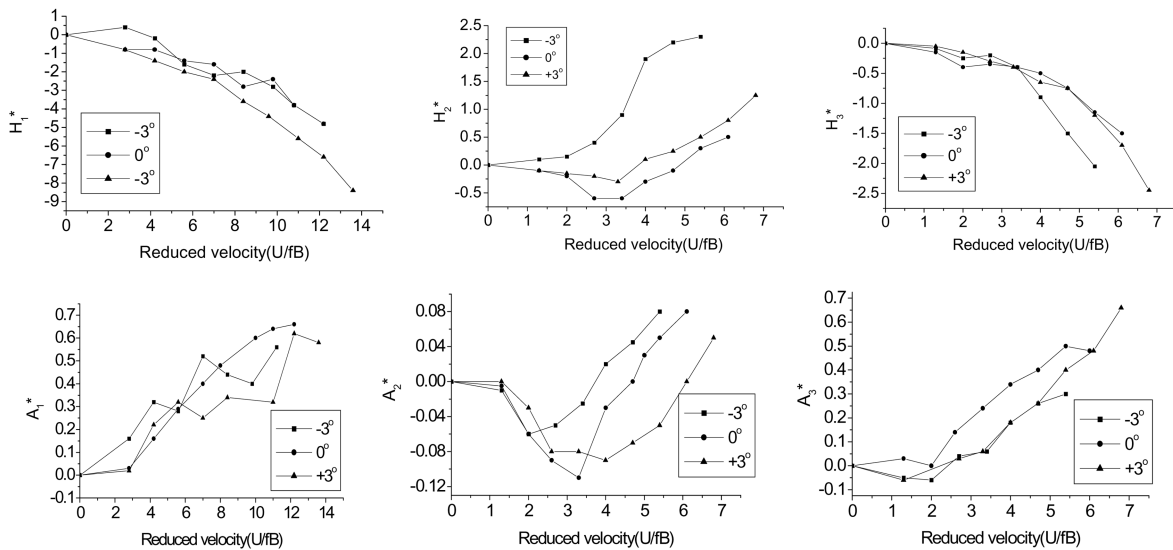

Fig. 12 Flutter derivatives at varying angles of wind incidence versus the reduced velocity

Table 5 Effect of cable materials on the critical wind speed (m/s)

Wind attack angle	Cable type	
	Steel	CFRP
$-3°$	75.5	75.0
$0°$	87.4	87.0
$+3°$	93.1	91.0

fundamental torsional frequency is very limited, it is less than the decrease of the coefficient C, so the critical wind speed is decreased. Viewed from the aspect of aerodynamic stability, the use of CFRP stay cables in long-span cable-stayed bridges is also feasible.

4. Conclusions

In this work, based on the Runyang Bridge and Jinsha Bridge, a suspension bridge using CFRP cables and a cable-stayed bridge using CFRP stay cables are schemed, in which the cable's cross-sectional area is determined by the principle of equivalent axial stiffness. The dynamic behavior, the aerostatic and aerodynamic stability of the two bridges using either CFRP or steel cables are investigated analytically, and some conclusions are drawn for the bridges with CFRP cables as follows:

(1) Due to the decrease of structural mass, structural natural frequencies are all increased, and particularly the torsional frequency is remarkably increased for suspension bridge.
(2) Under the static wind action, structural deformation is increased, however its aerostatic stability is basically remained the same as that of the bridge using steel cables.
(3) For suspension bridge, its aerodynamic stability is superior to the case with steel cables. But for cable-stayed bridge, its aerodynamic stability is basically the same as that of the case with steel stay cables.
(4) Considering the better wind resistance, the cable's cross-sectional area should be determined by the principle of equivalent axial stiffness.
(5) Viewed from the wind resistance, the use of CFRP cables in cable-supported bridges is feasible under the current span length. But for longer span, it needs to be further studied.

Acknowledgements

References

Astiz, M. A. (1998), "Flutter stability of very long suspension bridges", *J. Bridge Eng.*, *ASCE*, **3**(3), 132-139.
Chen, A. R. and Song, J. Z. (2000), "Wind-resistant study on the Runyang Bridge over the Yangtze River", Shanghai: *Res. Rep of Tongji University.*

Chen, S. H. (1999), "Structural and aerodynamic stability analysis of long-span cable-stayed bridges", Ph.D. thesis, Carleton University, Ottawa, Canada.

Gaubinger, B. and Kollegger, J. (2002), "Development of an anchorage system for CFRP tendons", *IABSE Symposium*, Melbourne.

Geffroy, R. L. (2002), "The Laroin footbridge with carbon composite stay cables", *Proceedings of the International Footbridge Conference*, Paris, France.

Hojo, T. and Noro, T. (2002), "Application of CFRP cables for cable-supported bridges", *IABSE Symposium*, Melbourne.

Kou, C. H., Xie, X., Gao, J. S. and Huang, J. Y. (2005), "Static behavior of long-span cable-stayed bridges using carbon fiber composite cable", *J. Zhejiang University(Engineering Science)*, **39**(1), 137-142.

Khalifa, M. A. (1992), "Dynamic vibration of cable-stayed bridges using carbon fiber composite cables", *Advanced Composite Materials in Bridges and Structures*, Neale, K. W., *et al.* (eds), CSCE.

Kim, P. and Meier, U. (1991), "CFRP cables for large structures", *Advanced Composites in Civil Engineering Structures*, Lyer, S. L. (ed), ASCE Specialty Conference, Las Vegas.

Kremmidas, S. C. (2004), "Improving bridge stay cable performance under static and dynamic loads", Ph.D. Dissertation, University of California, San Diego, America.

Meier, U. (1992), "Carbon fiber reinforced polymers: Modern materials in bridge engineering", *Struct. Eng. Int.*, IABSE, **1**, 7-12.

Meier, U. and Meier, M. (1996), "CFRP finds in cable support for bridges", *Modern Plastics*, 87-88.

Meier, U. (1999), "The use of carbon fiber reinforced polymer(CFRP) cables in bridge engineering", *Proceeding from the Techtextil Symposium*, Frankfurt.

Noistering, J. F. (2000), "Carbon fiber composites as stay cables for bridges", *Appl. Comp. Mater.*, **7**, 139-150.

Ohashi, M. (1991), "Cables for cable-stayed bridges", *Cable-Stayed Bridges: Recent Development and their Future*, Ito, M., *et al.* (eds), Elsevier Science Publishers, B.V.

Song, J. Z. (1998), "Wind-resistant study on the Jinsha Bridge over the Yangtze River", Shanghai: Res. Rep of Tongji University.

Xiang, H. F. and Ge, Y. J. (2002), "Refinements on aerodynamic stability analysis of super long-span bridges", *J. Wind Eng. Ind. Aerodyn.*, **90**, 1493-1515.

Xie, X., Gao, J. S., Kou, C. H. and Huang, J. Y. (2005), "Structural dynamic behavior of long-span cable-stayed bridges using carbon fiber composite cable", *J. Zhejiang University(Engineering Science)*, **39**(5), 728-733.

Zhang, X. J., Sun, B. N., and Xiang, H. F. (2002), "Nonlinear aerostatic and aerodynamic analysis of long-span suspension bridges considering wind-structure interactions", *J. Wind Eng. Ind. Aerodyn.*, **90**(9), 1065-1080.

CC